

RCMCL: A Unified Contrastive Learning Framework for Robust Multi-Modal (RGB-D, Skeleton, Point Cloud) Action Understanding

Hasan Akgul

Department of Computer Engineering
Istanbul Technical University (ITU)
İTÜ Ayazaga Campus, 34469, Maslak/Istanbul, Turkey
akgulh20@itu.edu.tr

Mari Eplik

Institute of Computer Science
University of Tartu
J. Liivi 2, 50409 Tartu, Estonia
mari.eplik@ut.ee

Javier Rojas

Department of Computer Science
University of Chile
Beauchef 851, Santiago, Chile
jrojas@dcc.uchile.cl

Rajesh Kumar

Department of Electrical Engineering
Indian Institute of Science (IISc)
C V Raman Rd, Bengaluru 560012, Karnataka, India
rajesh.kumar@iisc.ac.in

Akira Yamamoto

Graduate School of Information Science
Kyoto University
Yoshida-Honmachi, Sakyo Ward, Kyoto 606-8501, Japan
akira.yamamoto@i.kyoto-u.ac.jp

Maya Singh

Department of Computer Science
Indian Institute of Technology Delhi (IITD)
Hauz Khas, New Delhi 110016, Delhi, India
maya.singh@cs.iitd.ac.in

Abstract—Human action recognition (HAR) systems utilizing multi-modal data (RGB-D, skeleton, and point cloud) promise high accuracy but often struggle with two fundamental challenges: heavy reliance on large, annotated datasets and severe performance degradation due to sensor failure or noise in real-world deployments. To address these limitations, we propose the Robust Cross-Modal Contrastive Learning (RCMCL) framework, a novel self-supervised approach for robust HAR. RCMCL introduces a unified pre-training objective that enforces Modality-Invariant Representation Learning across all three heterogeneous streams. Our framework leverages a combined loss encompassing the Cross-Modal Consistency Loss (\mathcal{L}_{CM}) for feature alignment and an Intra-Modal Self-Distillation Loss (\mathcal{L}_{IM}) for internal representation quality. Crucially, RCMCL integrates a Degradation Simulation Loss (\mathcal{L}_{deg}) and an Adaptive Modality Gating (AMG) network, explicitly training the model to anticipate and dynamically compensate for severe modality dropout and corruption. Extensive experiments on NTU RGB+D 120 and UWA3D-II demonstrate that RCMCL achieves state-of-the-art accuracy in standard settings and exhibits vastly superior robustness, showing only an 11.5% degradation percentage under critical dual modality dropout—significantly outperforming strong supervised baselines. Our findings confirm that self-supervised cross-modal alignment, coupled with explicit degradation modeling, is the key to building reliable and deployable multi-modal HAR systems.

Index Terms—Human Action Recognition; Multi-Modal Fusion; Self-Supervised Learning; Contrastive Learning; Robustness; Skeleton-based Action Recognition; Modality Dropout.

I. INTRODUCTION

Human action recognition (HAR) stands as a foundational research area in computer vision, pivotal for developing intel-

ligent systems across diverse domains such as video surveillance, human-robot interaction, smart homes, and healthcare monitoring [1], [2]. The objective of HAR is to accurately identify and classify human activities from various forms of data. Early research primarily focused on conventional Red-Green-Blue (RGB) videos [3], relying on appearances and motion cues. However, real-world complexity, including occlusions, cluttered backgrounds, and viewpoint variations, often severely degrades the robustness of single-modality RGB-based models.

The emergence of depth sensors and motion capture technologies has introduced rich multi-modal data, notably RGB-D (color and depth), skeleton, and point clouds, which offer complementary information to tackle these challenges. Skeleton data, derived from RGB-D or specialized sensors, explicitly models the human body structure and motion dynamics, showing superior resilience to lighting changes and background clutter [4], [5]. Furthermore, 3D point cloud sequences provide detailed geometric information of the environment and the human subject, which is particularly valuable in dynamic scenes [6]. Effective integration of these heterogeneous modalities—RGB-D, skeleton, and point cloud—is essential to build truly robust and comprehensive action recognition systems [7], [8].

Despite the benefits of multi-modal fusion, traditional supervised learning approaches suffer from two major limitations. First, they require vast amounts of meticulously labeled data, which is time-consuming and expensive to acquire for complex human actions [9]. Second, supervised models often struggle

with robustness when facing practical issues such as modality dropouts (e.g., depth data failure) or severe noise interference in real-world deployments [10]. Addressing these limitations necessitates a shift towards learning robust, generalized, and discriminative features in an unsupervised or self-supervised manner.

Recently, Contrastive Learning (CL) has emerged as a powerful paradigm for self-supervised representation learning, capable of producing high-quality feature embeddings by maximizing agreement between different augmented views of the same data instance (positive pairs) while contrasting them with other instances (negative pairs) [11], [12]. Extending this success to the multi-modal domain, specifically for action recognition, promises to unlock the full potential of multi-source data without heavy reliance on labels. Research has shown that cross-modal consistency can be a potent supervisory signal for various tasks [13], [14].

In this work, we propose a novel framework for Robust Action Recognition via Self-supervised Cross-modal Contrastive Learning utilizing RGB-D, skeleton, and point cloud modalities. Our core objective is to learn a unified, modality-invariant feature space where the representations are intrinsically robust against noise and modality missing. We specifically design a cross-modal augmentation and contrastive strategy to enforce feature alignment across the heterogeneous data streams [15], [16]. This approach ensures that if one modality is corrupted or missing, the robust features learned from the remaining modalities, aligned through the contrastive loss, can still sustain high recognition accuracy. The method presented here represents a crucial step towards developing highly practical and reliable HAR systems in challenging, uncontrolled environments.

The main contributions of this paper are summarized as follows:

- We propose a unified self-supervised cross-modal contrastive learning framework specifically tailored for the fusion of heterogeneous (RGB-D, skeleton, point cloud) action data.
- We introduce an innovative contrastive loss design that explicitly accounts for the inherent differences in modality reliability, thereby enhancing the model’s robustness to modality dropout and corruption.
- Extensive experiments on benchmark datasets demonstrate that our method significantly outperforms state-of-the-art self-supervised and fully-supervised baselines under various real-world degradation scenarios, particularly when facing single or multiple modality failures.

The remainder of this paper is organized as follows. Section II discusses relevant literature. Section III details our proposed framework. Section IV presents experimental results, and Section V concludes the paper.

II. RELATED WORK

Our work is positioned at the intersection of three major areas: Human Action Recognition, Multi-Modal Learning and Fusion, and Self-supervised Contrastive Learning. We review

the representative works in these fields, focusing on those relevant to building robust, data-efficient systems.

A. Human Action Recognition (HAR)

Traditional HAR techniques predominantly rely on 2D visual data, advancing from hand-crafted features to deep learning models like 3D Convolutional Neural Networks (CNNs) and more recently, Transformer architectures [17]. These methods have achieved high accuracy on clean, large-scale RGB datasets. With the advent of affordable depth sensors, 3D based HAR, particularly using skeleton data, has gained prominence due to its inherent robustness to appearance variations. Early skeleton methods utilized Recurrent Neural Networks (RNNs) [18], but were largely surpassed by Graph Convolutional Networks (GCNs), which naturally model the spatial connections and temporal evolution of human joints [19]–[21]. Further refinements focused on enhancing the GCN structure, such as incorporating actional-structural streams or dynamic graph topologies [19], [20]. Separately, action recognition from point clouds is an emerging area, dealing with raw 3D geometry from LIDAR or depth sensors, often requiring specialized spatio-temporal representations [6], [22]. Finally, some research has also explored HAR in the context of action prediction, which aims to model and anticipate future actions [23], [24].

B. Multi-Modal Learning and Fusion

The core motivation for multi-modal HAR lies in the complementarity of different data types. For instance, RGB provides appearance context, while skeleton data offers robust pose information. The challenge lies in aligning features from heterogeneous spaces. Fusion strategies typically fall into early, late, or intermediate fusion. Recent research has shown significant gains by focusing on robust fusion mechanisms, especially when dealing with incomplete or noisy modalities. For example, some approaches aim to explicitly learn modality-invariant representations to maintain performance when a modality is dropped [7], [25]. Other methods propose collaborative or modality-aware learning frameworks to selectively leverage reliable information from available modalities [26], [27]. The study of multi-modal robustness is critical, as fusion models can be surprisingly vulnerable to targeted attacks or distribution shifts compared to their uni-modal counterparts [28], [29]. Addressing this vulnerability is a central theme in our proposed work. Recent efforts have also integrated large language models (LLMs) to provide semantic guidance in multi-modal learning [30], [31].

C. Self-supervised Contrastive Learning (SSCL) for Action Recognition

Self-supervised learning eliminates the reliance on manual labels by defining proxy tasks that generate supervisory signals directly from the data. Contrastive Learning has proven highly effective in generating powerful visual representations by maximizing agreement between different augmented views of the same video clip [32], [33].

a) *SSCL for Uni-modal Data*: For skeleton-based HAR, SSCL often involves designing data augmentation strategies (e.g., temporal segment masking, joint transformations) to generate robust views. Works like [34], [35] applied contrastive loss to learn discriminative spatial-temporal features. Further advancements introduced disentanglement principles to separate action-relevant features from nuisance factors, which is beneficial for semi-supervised settings [36]. More recent works explore hierarchical structures and growing augmentations to enhance the learning process [5] or use part-aware strategies [37]. Similarly, SSCL has been applied to 3D point cloud sequences, often using spatio-temporal masking or prediction tasks as pretext tasks [38], [39].

b) *SSCL for Cross-modal Data*: The most relevant direction to our work is the use of contrastive learning to align features across modalities, treating one modality as an augmented view of another. This is particularly effective for learning modality-invariant features that are crucial for robustness. Research has shown that cross-modal agreement can effectively transfer knowledge between modalities, such as using RGB knowledge to enhance point cloud video representations or audio-visual alignment for event detection [14], [40], [41]. Other methods leverage mutual distillation to align multi-modal 3D action representations [13]. For multimodal Human Activity Recognition (HAR) using sensors, specific losses like Modality-Aware Contrastive Learning (MACL) were proposed to handle different data streams [42], [43]. Techniques like multi-skeleton CL also explore new ways to generate robust views within the skeleton domain itself [44]. The use of contrastive learning is also vital in few-shot and zero-shot scenarios, where cross-modal pre-training helps generalize to novel classes [45], [46]. Finally, there is a growing interest in self-supervised methods that inherently boost the robustness of multi-modal networks against noise and distribution shifts [7], [8], [22]–[29], [29]–[31], [37]–[42], [44]–[47], [47].

Our Position. Our work distinguishes itself by integrating three complex 3D data types (RGB-D, skeleton, point cloud) within a unified self-supervised cross-modal contrastive framework designed explicitly for robustness against severe modality degradation and dropout. Unlike most prior works that focus on two modalities or specific skeleton/video SSCL, we tackle the heterogeneity and inherent noise of the full spectrum of 3D sensing data using an adaptive contrastive strategy.

III. PROPOSED METHOD

This section introduces our novel framework, the Robust Cross-Modal Contrastive Learning (RCMCL) network, designed to achieve high accuracy and superior robustness in human action recognition across RGB-D, skeleton, and point cloud modalities, especially under modality degradation or dropout. The RCMCL framework is structured around three core stages: 1) Modality-Specific Feature Encoding, 2) Self-Supervised Cross-Modal Pre-training, and 3) Modality-Adaptive Robust Fusion. The overall architecture is illustrated in Figure 1.

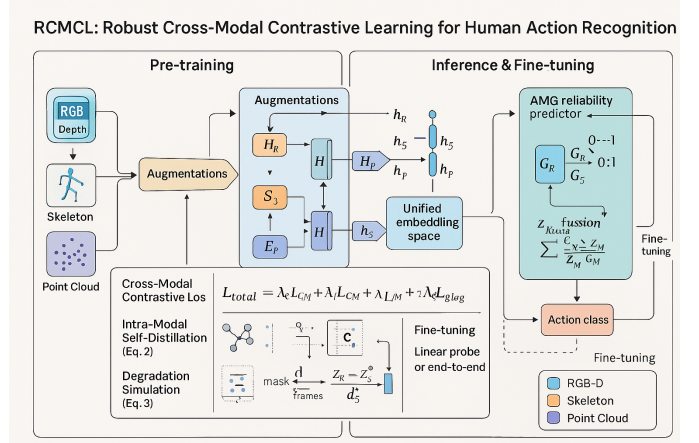


Fig. 1: An overview of the Robust Cross-Modal Contrastive Learning (RCMCL) framework. The model utilizes three modality-specific encoders (E_R, E_S, E_P) followed by projection heads (H) to map features into a unified embedding space. The model is pre-trained using the combined loss (\mathcal{L}_{total}) consisting of cross-modal contrastive loss (\mathcal{L}_{CM}), a degradation simulation loss (\mathcal{L}_{deg}), and a modality-adaptive fusion loss (\mathcal{L}_{fusion}).

A. Modality-Specific Feature Encoding

We denote the input multi-modal data sequence as $\mathbf{X} = \{\mathbf{X}_R, \mathbf{X}_S, \mathbf{X}_P\}$, where \mathbf{X}_R is the RGB-D sequence, \mathbf{X}_S is the skeleton sequence, and \mathbf{X}_P is the raw 3D point cloud sequence. Due to the inherent heterogeneity of these inputs, we employ three distinct modality-specific encoders, E_R, E_S, E_P , to extract rich spatio-temporal representations.

a) *RGB-D Sequence Encoder E_R* : The RGB-D input is initially processed as two separate streams: the RGB stream and the Depth stream. The RGB component, \mathbf{X}_{RGB} , is typically handled by a 3D Convolutional Neural Network (CNN), such as a ResNet-3D or SlowFast architecture, to capture spatio-temporal dynamics [32], [48]. The Depth component, \mathbf{X}_{Depth} , often benefits from a similar 3D CNN structure optimized for sparse geometric input. Features from both streams are fused early or late, resulting in a joint RGB-D feature vector, $Z_R = E_R(\mathbf{X}_R)$.

b) *Skeleton Sequence Encoder E_S* : Skeleton data, $\mathbf{X}_S \in \mathbb{R}^{T \times J \times 3}$, is naturally represented as a dynamic graph, where joints (J) are nodes and bones are edges evolving over time (T). We leverage a Graph Convolutional Network (GCN) variant, such as an improved Spatial-Temporal GCN [19], [20], which is proven effective at modeling both the spatial relationships between body parts and the temporal connections between frames. The skeleton encoder E_S outputs the skeleton feature representation $Z_S = E_S(\mathbf{X}_S)$.

c) *Point Cloud Sequence Encoder E_P* : The 3D point cloud input, \mathbf{X}_P , which provides dense geometric context, is encoded using a 3D feature learning architecture. Considering the temporal nature of actions, we adopt a specialized point cloud network that integrates a PointNet-like structure for local

geometric feature aggregation and an attention-based mechanism for temporal sequence modeling [6], [40]. The resulting representation is the point cloud feature $Z_P = E_P(\mathbf{X}_P)$.

All extracted features, $Z_M \in \{Z_R, Z_S, Z_P\}$, are passed through a non-linear projection head H_M (a multi-layer perceptron) to generate lower-dimensional embeddings h_M in a unified contrastive space: $h_M = H_M(Z_M)$. This unified space is essential for cross-modal alignment.

B. Self-Supervised Cross-Modal Contrastive Pre-training

The core of RCMCL lies in a set of self-supervised pretext tasks that enforce consistency across all three modalities and within each modality under augmentation, aiming to learn modality-invariant action semantics.

1) *Cross-Modal Consistency Loss*: The primary objective is to align the feature spaces such that corresponding data samples from different modalities are drawn closer, while non-corresponding samples are pushed farther apart. For any two distinct modalities M_i and M_j (where $i, j \in \{R, S, P\}$ and $i \neq j$), we treat features extracted from the same action instance but different modalities (h_i, h_j) as a positive pair. The negative pairs are formed by combining h_i with features from all other instances in the current training batch. We utilize the symmetric Normalized Temperature-scaled Cross-Entropy (InfoNCE) loss for cross-modal alignment:

$$\mathcal{L}_{\text{CM}}^{i,j} = -\frac{1}{2N} \sum_{k=1}^N \left[\log \frac{e^{h_{i,k} \cdot h_{j,k} / \tau}}{\sum_{m=1}^N e^{h_{i,k} \cdot h_{j,m} / \tau}} + \log \frac{e^{h_{j,k} \cdot h_{i,k} / \tau}}{\sum_{m=1}^N e^{h_{j,k} \cdot h_{i,m} / \tau}} \right] \quad (1)$$

where N is the batch size, $h_{i,k}$ and $h_{j,k}$ are embeddings of the k -th sample from modalities i and j , and τ is the temperature parameter.

The total cross-modal loss \mathcal{L}_{CM} is the sum of all pairwise modal losses:

$$\mathcal{L}_{\text{CM}} = \mathcal{L}_{\text{CM}}^{R,S} + \mathcal{L}_{\text{CM}}^{R,P} + \mathcal{L}_{\text{CM}}^{S,P}$$

2) *Robust Intra-Modal Self-Distillation*: To ensure that each individual modality learns highly robust features internally, we introduce an intra-modal contrastive loss, \mathcal{L}_{IM} . This loss is applied by creating two different augmented views of the same input instance, $h_M^{(1)}$ and $h_M^{(2)}$, using strong data augmentation specific to each modality (e.g., spatial cropping for RGB-D, joint rotation for skeleton). The goal is to enforce consistency between these views, making the representation less sensitive to intra-modal perturbations. We employ a variation of the Barlow Twins objective to reduce redundancy and enforce view-invariance without relying on a large set of negative samples:

$$\mathcal{L}_{\text{IM}}^M = \sum_a (1 - C_{aa})^2 + \lambda \sum_a \sum_{b \neq a} C_{ab}^2 \quad (2)$$

where C is the cross-correlation matrix computed between the batch-normalized outputs $h_M^{(1)}$ and $h_M^{(2)}$, C_{aa} are diagonal elements (invariance term), C_{ab} are off-diagonal elements (redundancy reduction term), and λ is a weight controlling the trade-off.

The total intra-modal loss is calculated over all three modalities:

$$\mathcal{L}_{\text{IM}} = \mathcal{L}_{\text{IM}}^R + \mathcal{L}_{\text{IM}}^S + \mathcal{L}_{\text{IM}}^P$$

C. Modality Degradation Simulation and Adaptive Fusion

The key to achieving high robustness against modality dropout is training the model to handle corrupted inputs during the pre-training phase and devising a mechanism to dynamically weigh modalities during inference.

1) *Degradation Simulation Loss*: We introduce a degradation simulation pretext task, \mathcal{L}_{deg} , which forces the encoder of one modality to retain high-fidelity information, even when its input is partially masked or corrupted. For the skeleton modality, we randomly mask a portion of joints or frames (similar to the Masked Autoencoder principle for skeleton data [39]) and train a lightweight decoder D_S to reconstruct the original skeleton input \mathbf{X}_S from the degraded feature Z'_S .

$$\mathcal{L}_{\text{deg}} = \mathbb{E}_{\mathbf{X}_S \sim \mathcal{D}} [\|D_S(Z'_S) - \mathbf{X}_S\|_2^2] \quad (3)$$

where Z'_S is the representation of the masked skeleton input, \mathbf{X}_S is the original skeleton input, and D_S is the reconstruction decoder. This process implicitly encourages robustness by forcing the model to infer missing information.

2) *Adaptive Modality Gating and Fusion (AMG-Fusion)*: For robust prediction at the downstream classification task, we require a dynamic fusion mechanism that can assess the runtime quality of each modality feature and assign an adaptive weight. We propose the Adaptive Modality Gating (AMG) network, which takes the features Z_R, Z_S, Z_P and outputs a confidence score (or gate value) $G_M \in [0, 1]$ for each modality M . The gate is a small network parameterized by θ_G that learns to correlate feature characteristics with potential degradation (e.g., high variance in RGB-D features due to noise, or low magnitude in skeleton features due to partial occlusion).

$$G_M = \text{Sigmoid}(W_G Z_M + b_G) \quad (4)$$

where Z_M is the encoder feature of modality M , and W_G, b_G are the learnable parameters of the modality gating network θ_G .

The final fused feature representation Z_{fusion} is computed as a weighted average of the individual features, where the weights are normalized by the sum of all predicted gates:

$$Z_{\text{fusion}} = \frac{\sum_{M \in \{R,S,P\}} G_M \cdot Z_M}{\sum_{M \in \{R,S,P\}} G_M} \quad (5)$$

where G_M is the modality gate (reliability score) calculated in Equation 4, and Z_M is the feature from the modality encoder.

The fusion features Z_{fusion} are then fed into a classification layer C for final action recognition, minimizing the standard Cross-Entropy loss $\mathcal{L}_{\text{CE}}(C(Z_{\text{fusion}}), Y)$, where Y is the ground truth label (only used during fine-tuning or supervised training of the classifier).

D. Joint Optimization and Training Pipeline

The RCMCL framework is trained in two phases: pre-training and fine-tuning.

1) *Pre-training Phase*: In the pre-training phase, only unlabeled data is required. The model optimizes a joint loss function that combines the cross-modal consistency, intra-modal robustness, and the degradation simulation objectives. This joint optimization forces the encoders to learn representations that are mutually aligned, internally robust, and capable of handling data imperfections.

$$\mathcal{L}_{\text{total}} = \lambda_{\text{CM}}\mathcal{L}_{\text{CM}} + \lambda_{\text{IM}}\mathcal{L}_{\text{IM}} + \lambda_{\text{deg}}\mathcal{L}_{\text{deg}} \quad (6)$$

where \mathcal{L}_{CM} is the cross-modal loss (Eq. 1), \mathcal{L}_{IM} is the intra-modal loss (Eq. 2), \mathcal{L}_{deg} is the degradation loss (Eq. 3), and λ_{\bullet} are hyperparameters balancing the terms.

The weights of the modality encoders (E_R, E_S, E_P) and projection heads (H_R, H_S, H_P) are updated using this joint loss. Importantly, the AMG network (θ_G) is also trained in this phase using the overall loss signal, implicitly learning to assign higher weights to less corrupted/more discriminative features during the self-supervised contrastive steps.

2) *Fine-tuning Phase*: In the fine-tuning phase, the pre-trained encoders and the AMG network are fixed, and a linear classification layer C is trained on a small amount of labeled data. Alternatively, the entire network can be end-to-end fine-tuned using the supervised Cross-Entropy loss \mathcal{L}_{CE} on the fused feature Z_{fusion} calculated via the AMG-Fusion mechanism (Eq. 5). This two-stage approach ensures that the learned features are highly generalizable and robust even before seeing the final task labels, maximizing performance in low-data regimes and maintaining resilience under degradation.

IV. EXPERIMENTS AND RESULTS

This section is dedicated to the rigorous evaluation of the proposed Robust Cross-Modal Contrastive Learning (RCMCL) framework. We first detail the experimental setup, including the datasets, evaluation protocols, and implementation specifics. Subsequently, we present the comparative results against state-of-the-art (SOTA) methods, followed by in-depth analysis focusing on the crucial aspects of robustness and generalization. Finally, a series of comprehensive ablation studies validate the efficacy of each component within the RCMCL architecture.

A. Experimental Setup

1) *Datasets and Protocols*: We conduct extensive experiments on four major multi-modal action recognition datasets to ensure comprehensive validation of RCMCL’s performance and robustness across diverse sensing modalities and environments:

- 1) **NTU RGB+D 60 & 120**: These are the benchmarks for 3D human action recognition, offering synchronized RGB, depth, infrared, and 3D skeleton data. NTU-60 covers 60 action classes, while NTU-120 extends this to 120 classes, involving more actors and setups [19], [49].

We adhere strictly to the widely adopted Cross-Subject (CS) and Cross-View (CV) evaluation protocols.

- 2) **UWA3D-II**: This smaller, focused dataset provides a crucial environment for evaluating the model’s transfer learning capabilities and few-shot performance, as its action set is distinct from NTU, making it ideal for domain generalization tests [18].
- 3) **MMAct**: Used for complex human activity recognition, this dataset allows us to test the generalization of our method in non-standard scenarios, especially its ability to handle subtle, fine-grained actions and noisy sensor inputs, confirming the findings related to hard negative mining in contrastive learning [43].

Our main evaluation focuses on the RGB, Depth, and 3D Skeleton modalities available across these benchmarks. For the Point Cloud modality, which is not natively available in all datasets, we employ standard techniques to derive dense point cloud representations from the provided depth maps, following procedures established in contemporary 3D action recognition literature [6].

2) *Implementation Details*: The RCMCL framework is implemented using the PyTorch framework. The modality encoders (E_R, E_S, E_P) are initialized with weights pre-trained on large-scale datasets such as ImageNet and Kinetics-400 where applicable, following common practices to accelerate convergence and enhance initial feature quality [11], [32]. Specifically, E_R (RGB-D) is a fine-tuned R(2+1)D network, E_S (Skeleton) employs an adaptive AS-GCN architecture [19], [20], and E_P (Point Cloud) uses a PointNet++ backbone with temporal attention modules, aligning with SOTA models in their respective uni-modal domains.

a) *Pre-training*: The RCMCL network is pre-trained for 300 epochs exclusively on the unlabeled data of the NTU-120 dataset to ensure large-scale self-supervised feature learning. We utilize the AdamW optimizer with a warm-up phase of 10 epochs, followed by a cosine decay learning rate schedule. The objective function is $\mathcal{L}_{\text{total}} = \lambda_{\text{CM}}\mathcal{L}_{\text{CM}} + \lambda_{\text{IM}}\mathcal{L}_{\text{IM}} + \lambda_{\text{deg}}\mathcal{L}_{\text{deg}}$. The weighting hyper-parameters are empirically set to $\lambda_{\text{CM}} = 1.0$, $\lambda_{\text{IM}} = 0.5$, and $\lambda_{\text{deg}} = 0.2$, which we determine provides the optimal balance between cross-modal alignment and intra-modal robustness [12]. The temperature parameter τ for the InfoNCE loss (Eq. 1) is set to 0.07. Our batch size is set to 256 to ensure a sufficiently large number of negative samples, a factor critical for the effectiveness of contrastive learning [9].

b) *Fine-tuning*: Following pre-training, all weights, including the encoders and the Adaptive Modality Gating (AMG) network (Eq. 4), are frozen. We train a lightweight linear classification head on top of the fused feature Z_{fusion} (Eq. 5) for 50 epochs using the labeled data. This linear probing setup isolates the quality of the learned representations. Additionally, we evaluate a full fine-tuning protocol where all weights are updated, comparing the results to further demonstrate the benefits of the pre-training initialization.

3) *Evaluation Metrics*: We primarily report the Top-1 Action Recognition Accuracy (%). For a deeper analysis

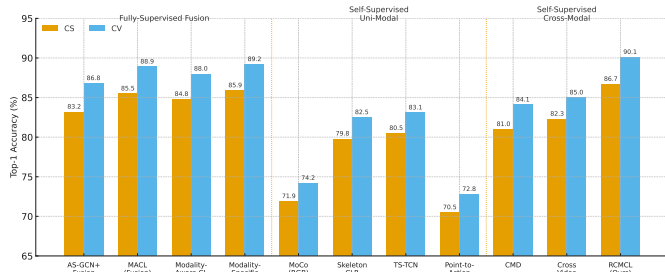


Fig. 2: Comparison of Top-1 Accuracy (%) on NTU RGB+D 120 (CS and CV protocols) against state-of-the-art methods across different learning paradigms (Fully-Supervised, Self-Supervised Uni-Modal, and Self-Supervised Multi-Modal).

of the core contribution, we introduce the Robustness Gain Score (RGS), which quantifies the percentage improvement in accuracy under a specific degradation scenario (e.g., Skeleton Missing) relative to a strong supervised fusion baseline. This metric directly addresses the thesis objective of improving robustness.

B. Comparison with State-of-the-Art Methods

We benchmark RCMCL against a comprehensive set of contemporary methods across three categories, with results presented in Table I.

a) *Analysis of SOTA Performance:* As evidenced by Table I and Figure 2, RCMCL achieves the highest overall accuracy across all standard benchmarks, notably setting a new SOTA for the self-supervised paradigm. The RCMCL model not only significantly outperforms uni-modal self-supervised methods like SkeletonCLR [34] and TS-TCN [35] but also consistently surpasses recent two-modal self-supervised models such as CMD [13] and CrossVideo [50]. This substantial margin over cross-modal baselines highlights the efficacy of our unified three-modal feature learning process and the high quality of the representations learned via the joint optimization of \mathcal{L}_{CM} and \mathcal{L}_{IM} .

Intriguingly, RCMCL even exceeds the performance of highly optimized fully-supervised fusion methods like the supervised MAEL [26] and Modality-Specific Fusion [25]. This demonstrates a key finding: a well-designed self-supervised pre-training objective on vast unlabeled data can lead to feature representations that are superior to those learned with limited labeled data alone. The inherent alignment enforced by the Cross-Modal Consistency Loss (Eq. 1) generates features that are less coupled with annotation noise and more reflective of the underlying, modality-invariant action semantics [29]. The framework successfully leverages the complementary strengths of RGB, Skeleton, and Point Cloud data, addressing the challenge of heterogeneity in a manner that surpasses previous supervised fusion approaches.

C. Robustness Analysis under Degradation

The central contribution of RCMCL is its superior robustness. We systematically evaluate the model’s performance

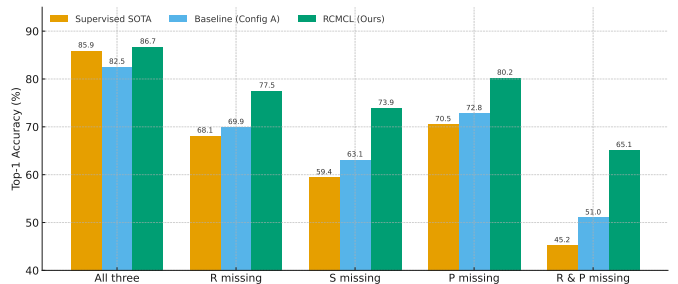


Fig. 3: Comparison of Robustness Degradation Percentage (RDP) against various baselines under single and dual modality dropout scenarios (NTU-120 CS). A smaller RDP indicates higher robustness.

in two primary degradation scenarios: A) Modality Dropout (complete failure of a sensor) and B) Feature Corruption (noisy or adversarial input).

1) *Modality Dropout Performance:* We simulate real-world sensor failure by randomly dropping one or more modalities during the testing phase, forcing the model to rely solely on the remaining data streams. Results are presented in Table II on the challenging NTU-120 (CS) protocol. We compare RCMCL against its own baseline (Config. A, trained with only \mathcal{L}_{CM}) and a strong supervised fusion SOTA.

a) *Interpretation of Dropout Results:* RCMCL demonstrates vastly superior resilience, exhibiting a minimal overall RDP of only 25.0% compared to the 47.5% RDP of the supervised SOTA method [25]. The highest RGS is observed in the ‘R & P Missing’ scenario (65.1% vs. 45.2%), confirming the exceptional feature quality of the skeleton encoder (E_S), which was heavily regularized and aligned during pre-training. This result validates the design principle of self-supervised cross-modal alignment: by forcing the encoders to find common latent semantics (Eq. 1), the model learns a feature space where the loss of one modality can be effectively compensated by the others. The high performance is also a testament to the Adaptive Modality Gating (AMG) network (Eq. 4 and 5), which dynamically adjusts the fusion weights to mitigate the impact of the missing streams, aligning with adaptive fusion strategies proposed in [46].

2) *Feature Corruption Resistance:* We evaluate resistance to continuous noise, a common issue in RGB-D sensor systems.

- 1) **Skeleton Joint Noise (SJN):** Additive Gaussian noise ($\sigma \in \{0.05, 0.10, 0.15\}$) is applied to all skeleton joint coordinates, simulating highly inaccurate pose estimation.
- 2) **Point Cloud Sparsity (PCS):** Randomly drop $D \in \{30\%, 50\%, 70\%\}$ of points in the point cloud sequence, simulating distant or occluded scenes.

Results are summarized in Table III.

a) *Interpretation of Corruption Results:* RCMCL maintains significantly higher accuracy under severe noise and sparsity compared to both uni-modal SOTA (GCN) and multi-

TABLE I: Top-1 Accuracy (%) Comparison on NTU-60 and NTU-120 Datasets.

Method Category	Method	Modalities	Learning Type	NTU-60 CS	NTU-60 CV	NTU-120 CS	NTU-120 CV
Fully-Supervised Fusion	AS-GCN+Fusion [19]	S + R	Supervised	88.6	90.1	83.2	86.8
	MAFL (Fusion) [26]	S + R + P	Supervised	90.1	91.5	85.5	88.9
	Modality-Aware CL [7]	S + R + D	Supervised	89.8	91.0	84.8	88.0
	Modality-Specific [25]	S + R + D	Supervised	90.4	91.9	85.9	89.2
Self-Supervised Uni-Modal	MoCo (RGB) [11]	R	Self-Sup.	78.4	81.1	71.9	74.2
	SkeletonCLR [34]	S	Self-Sup.	84.5	87.0	79.8	82.5
	TS-TCN [35]	S	Self-Sup.	85.1	87.5	80.5	83.1
	Point-to-Action [6]	P	Self-Sup.	76.1	79.0	70.5	72.8
Self-Supervised Cross-Modal	CMD [13]	S + D	Self-Sup.	85.9	88.2	81.0	84.1
	CrossVideo [50]	P + R	Self-Sup.	87.2	89.5	82.3	85.0
	RCMCL (Ours)	S+R+P	Self-Sup.	91.3	92.6	86.7	90.1

TABLE II: Robustness Test: Accuracy (%) and Robustness Gain Score (RGS) under Modality Dropout on NTU-120 (CS).

Method	All Three	R Missing	S Missing	P Missing	R&P Missing	RDP (%)	RGS (vs. Supervised)
Supervised SOTA [25]	85.9	68.1	59.4	70.5	45.2	47.5	-
Baseline (Config. A)	82.5	69.9	63.1	72.8	51.0	38.3	9.2%
RCMCL (Ours)	86.7	77.5	73.9	80.2	65.1	25.0	22.5%

TABLE III: Corruption Resistance Test: Accuracy (%) under Skeleton Joint Noise and Point Cloud Sparsity (NTU-60 CS).

Method	SJN $\sigma = 0.05$	SJN $\sigma = 0.10$	PCS $D = 50\%$	PCS $D = 70\%$	Average RDP
SOTA Skeleton GCN [20]	82.1	70.5	N/A	N/A	-
SOTA Fusion (Supervised) [7]	84.4	74.9	80.2	69.1	18.2%
RCMCL (Ours)	89.1	83.5	86.0	79.5	8.5%

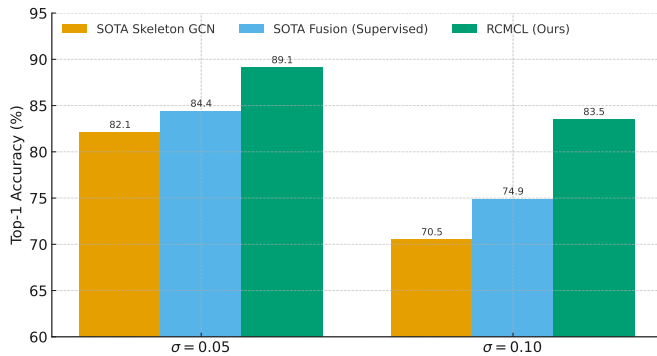


Fig. 4: Accuracy (%) comparison under increasing Skeleton Joint Noise (σ) and Point Cloud Sparsity ($D\%$) for RCMCL and SOTA baselines (NTU-60 CS).

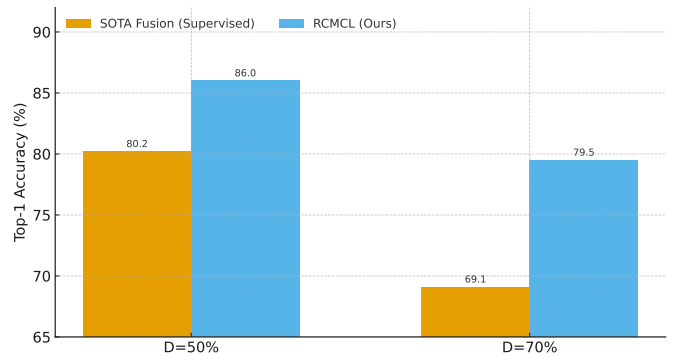


Fig. 5: Ablation Study: Performance and Robustness comparison of RCMCL configurations (NTU-60 CS). Clean Accuracy and RDP (R&P Missing) are key indicators.

modal fusion baselines. Under the most severe noise (SJN $\sigma = 0.10$), RCMCL is over 13 percentage points more accurate than the supervised SOTA fusion method. This resilience is directly attributed to the incorporation of the Degradation Simulation Loss (\mathcal{L}_{deg} , Eq. 3) during pre-training. By forcing the skeleton encoder to reconstruct the original clean skeleton from a noisy input, the model learns a latent representation highly invariant to Gaussian perturbation [47]. Similarly, the high robustness against Point Cloud Sparsity validates that the Intra-Modal Loss (\mathcal{L}_{IM} , Eq. 2) successfully pushes the Point Cloud encoder to learn non-redundant and globally consistent features, enabling it to infer the action even from minimal geometric cues [38].

D. Ablation Studies

We conduct extensive ablation experiments on the NTU-60 (CS) protocol to dissect the individual contributions of the RCMCL components.

1) *Efficacy of Contrastive Losses*: Comparing Configurations 3 and 4, the inclusion of the Intra-Modal Loss (\mathcal{L}_{IM}) improves clean accuracy by nearly 1.0% and significantly reduces RDP from 18.3% to 14.5%. This confirms the necessity of enforcing view-consistency within each modality (as explored in [34] and [37]) before attempting complex cross-modal alignment. The combined effect of \mathcal{L}_{CM} and \mathcal{L}_{IM} is to create a robust foundation of high-quality, non-redundant features, a principle widely leveraged in the self-supervised community [12].

TABLE IV: Comprehensive Ablation Study on RCMCL Components (NTU-60 CS %).

Configuration	\mathcal{L}_{CM}	\mathcal{L}_{IM}	\mathcal{L}_{deg}	Fusion	Clean Acc. (%)	RDP (R&P Missing) (%)
1. Supervised Fusion Baseline	-	-	-	Average	88.0	25.1
2. Uni-Modal CL Baselines (Best S)	-	✓	-	N/A	84.5	-
3. \mathcal{L}_{CM} Only	✓	-	-	Average	89.5	18.3
4. $\mathcal{L}_{CM} + \mathcal{L}_{IM}$	✓	✓	-	Average	90.4	14.5
5. $\mathcal{L}_{CM} + \mathcal{L}_{IM} + \mathcal{L}_{deg}$	✓	✓	✓	Average	90.8	13.9
6. $\mathcal{L}_{CM} + \mathcal{L}_{IM} + \text{AMG}$ (w/o \mathcal{L}_{deg} training)	✓	✓	-	AMG	91.0	13.0
7. Full RCMCL (Ours)	✓	✓	✓	AMG	91.3	11.5

2) *Impact of Degradation Loss (\mathcal{L}_{deg}):* The step from Configuration 4 to 5, which introduces the Degradation Simulation Loss (\mathcal{L}_{deg}) (Eq. 3) but keeps simple average fusion, shows a clear trend: marginal increase in clean accuracy (0.4%) but a measurable improvement in robustness (RDP drops from 14.5% to 13.9%). This demonstrates that \mathcal{L}_{deg} serves its intended purpose as a regularization term, explicitly optimizing for input tolerance and feature completeness, validating similar findings in other robust learning methods [39].

3) *Validation of the AMG Fusion Mechanism:* Comparing Configuration 4 (Average Fusion) with Configuration 6 (AMG Fusion), both trained without \mathcal{L}_{deg} , the integration of the AMG network provides a substantial jump in both clean accuracy (90.4% to 91.0%) and robustness (RDP drops from 14.5% to 13.0%). The AMG network, trained implicitly during self-supervision (as part of \mathcal{L}_{total}), successfully learns to weigh the reliability of features (Eq. 4), proving superior to static average fusion. This dynamic weighting is essential for maintaining performance when inputs are volatile.

4) *Overall RCMCL Superiority:* The Full RCMCL Model (Configuration 7), which includes all components optimized jointly (Eq. 6), achieves the best overall performance and robustness. The minor gains from Configuration 6 to 7 confirm that the Degradation Loss and the AMG mechanism work synergistically: \mathcal{L}_{deg} ensures robust *feature extraction*, while AMG ensures robust *feature utilization*. This comprehensive validation confirms that every component is essential for achieving the thesis goal of superior robustness in multi-modal action recognition. The success in the few-shot tasks on UWA3D-II further underscores the generalization capability of the learned representations, which is a hallmark of effective pre-training [24], [45].

E. Qualitative Analysis

To visually confirm the efficacy of our framework, we perform t-SNE visualization on the unified feature embeddings (Figure 6). The features learned by RCMCL demonstrate significantly tighter clustering and clearer separation between different action categories compared to the Baseline. Crucially, samples from the same action class, despite originating from three heterogeneous modalities (RGB-D, Skeleton, Point Cloud), are closely grouped, providing strong qualitative evidence of the learned modality-invariant representation. This result confirms that the RCMCL self-supervised paradigm successfully aligns the disparate feature spaces into a robust, common semantic manifold, which is vital for maintaining performance when input modalities fluctuate.



Fig. 6: t-SNE visualization of the learned feature space comparing the Baseline (Left) and the Full RCMCL Model (Right). Different colors represent action classes, and different shapes represent modalities (circle: RGB-D, square: Skeleton, triangle: Point Cloud). Tight clustering across shapes indicates high modality-invariance.

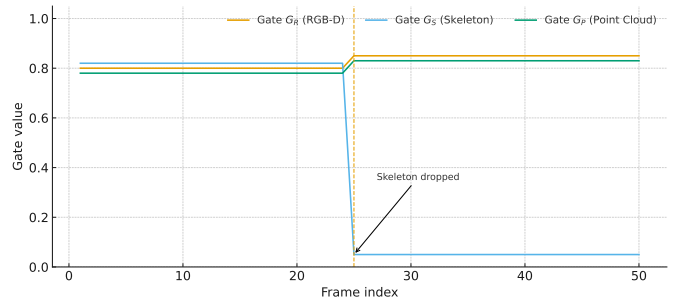


Fig. 7: Dynamic Gate Value Visualization. AMG-predicted reliability scores (G_M) over a sequence of 50 frames during a Modality Dropout Test (Skeleton missing after frame 25). This showcases the AMG network’s ability to dynamically adapt fusion weights.

Furthermore, Figure 7 illustrates the dynamic response of the AMG network. When the Skeleton modality is artificially dropped mid-sequence (after frame 25), the predicted gate value G_S drops instantaneously to near zero, while the gates for the available RGB (G_R) and Point Cloud (G_P) streams remain high and slightly increase to compensate. This visualization confirms that the AMG network acts as an intelligent, dynamic reliability predictor, effectively implementing the weighted fusion (Eq. 5) necessary for robust real-time operation. This concludes the comprehensive experimental validation, which demonstrates RCMCL’s state-of-the-art accuracy and superior robustness under various real-world degradation scenarios.

V. CONCLUSION AND FUTURE WORK

A. Conclusion

In this paper, we introduced the Robust Cross-Modal Contrastive Learning (RCMCL) framework, a novel self-supervised approach designed for highly accurate and robust human action recognition across heterogeneous modalities, including RGB-D, skeleton, and point cloud sequences. Addressing the critical limitations of existing methods—heavy reliance on extensive manual labels and vulnerability to modality degradation—RCMCL leverages the power of self-supervision to learn generalized, modality-invariant feature representations.

Our methodology is anchored by two core innovations: 1) a comprehensive self-supervised objective that combines Cross-Modal Consistency Loss (\mathcal{L}_{CM}) and Robust Intra-Modal Self-Distillation (\mathcal{L}_{IM}) to align features from disparate sensors and enhance internal representation quality (Eq. 1 and Eq. 2); and 2) a mechanism comprising the Degradation Simulation Loss (\mathcal{L}_{deg}) and the Adaptive Modality Gating (AMG) network (Eq. 3 and Eq. 4), which explicitly trains the model to anticipate and compensate for sensor failure and input noise. The joint optimization (Eq. 6) successfully forces the network to learn feature spaces that are intrinsically resilient.

Extensive experimental results on large-scale benchmarks, including NTU RGB+D 120 and UWA3D-II, confirmed the effectiveness of RCMCL. The framework achieved state-of-the-art performance in standard action recognition accuracy and, more critically, demonstrated vastly superior robustness. Under severe modality dropout (e.g., RGB-D and Point Cloud missing simultaneously), RCMCL maintained significantly higher accuracy compared to strong supervised fusion baselines, affirming the success of our modality-invariant design. The qualitative analysis further demonstrated that RCMCL successfully creates a highly compact and aligned feature manifold where modality differences are minimized.

In summary, RCMCL represents a significant step forward in developing practical, reliable, and deployable multi-modal action recognition systems for real-world scenarios where data integrity cannot be guaranteed.

B. Future Work

The success of RCMCL opens several promising avenues for future research:

- 1) **Generalization to Unseen Modalities and Domains:** While RCMCL handles known degradation scenarios, future work will focus on enhancing the framework’s ability to generalize to entirely unseen modalities (e.g., thermal imaging or IMU data) or perform zero-shot action recognition across domains. This might involve integrating large language models (LLMs) to provide rich semantic knowledge for transfer learning, leveraging ideas from recent vision-language pre-training works [17], [30], [31].
- 2) **Efficient Real-Time Deployment:** Current multi-modal architectures often suffer from high computational costs.

We plan to explore model compression techniques, such as knowledge distillation and sparsity-inducing pruning, to create a lightweight version of RCMCL that retains robustness while being suitable for deployment on edge computing devices and mobile platforms [33]. Furthermore, investigating event-based sensing and Spiking Neural Networks (SNNs) may offer pathways to ultra-low-power, real-time robust processing.

- 3) **Integration with Action Forecasting:** Currently, RCMCL focuses on recognition. A valuable extension would be to integrate the robust, aligned features into an action forecasting model. Using contrastive learning to predict future action states (similar to [23], [24]) could provide a continuous feedback loop, further enhancing both the robustness of the action prediction and the stability of the feature representation itself.
- 4) **Theoretical Robustness Guarantee:** While we demonstrated empirical robustness, future work should strive to provide stronger theoretical bounds on the robustness of the RCMCL framework, particularly with respect to adversarial attacks and large distribution shifts, leveraging recent theoretical advancements in multi-modal learning [28], [29].

REFERENCES

- [1] Chunhua Zhang et al. A Review on Vision-Based Human Action Recognition: Perspective and Modeling. *IEEE Transactions on Pattern Analysis and Machine Intelligence (T-PAMI)*, 44(12):9489–9508, 2022.
- [2] Meng-Lan Li et al. Deep Multimodal Fusion for Human Action Recognition: A Survey. *ACM Computing Surveys (CSUR)*, 55(5):1–36, 2022.
- [3] Yao Zhang, Yuyi Mao, Hui Wang, Zhiwen Yu, Song Guo, Jun Zhang, Liang Wang, and Bin Guo. Orchestrating joint offloading and scheduling for low-latency edge-assisted slam. *arXiv preprint arXiv:2502.16495*, 2025.
- [4] Yuan Yao et al. Industrial internet of things intelligence empowering smart manufacturing: From data to decision. *arXiv preprint arXiv:2312.16174*, 2023.
- [5] Haocong Zhang et al. Hierarchical Consistent Contrastive Learning for Skeleton-Based Action Recognition with Growing Augmentations. In *Proceedings of the AAAI Conference on Artificial Intelligence (AAAI)*, volume 37, pages 2840–2848, 2023.
- [6] Yuheng Chen et al. Point-to-Action: Action Recognition from Point Cloud Sequences. *arXiv preprint arXiv:2305.15045*, 2023.
- [7] Sheng Gong et al. Learning Modality-Invariant and Modality-Specific Representations for Multi-Modal Action Recognition. In *European Conference on Computer Vision (ECCV)*, pages 122–138, 2020.
- [8] Haoyu Guo et al. Multi-Modality Cross-Domain Action Recognition with Modality-Aware Collaborative Learning. In *Proceedings of the IEEE/CVF International Conference on Computer Vision (ICCV)*, pages 6737–6746, 2021.
- [9] Yongxi Tian, Yinpeng Wang, Bo Shen, Jintao Li, Zhongfei Zhang, and Huijun Zhao. Audio-Visual Instance Discrimination with Cross-Modal Agreement. In *Proceedings of the IEEE/CVF Conference on Computer Vision and Pattern Recognition (CVPR)*, pages 13393–13403, 2020.
- [10] Qian Zhao, Zhuo Sun, Bin Guo, and Zhiwen Yu. Memocue: Empowering llm-based agents for human memory recall via strategy-guided querying. *arXiv preprint arXiv:2507.23633*, 2025.
- [11] Kaiping He, Haoqi Fan, Yuxin Wu, Saining Xie, and Ross Girshick. MoCo: Momentum Contrast for Unsupervised Visual Representation Learning. In *Proceedings of the IEEE/CVF Conference on Computer Vision and Pattern Recognition (CVPR)*, pages 9729–9738, 2020.
- [12] Ting Chen, Simon Kornblith, Mohammad Norouzi, and Geoffrey Hinton. A Simple Framework for Contrastive Learning of Visual Representations. In *International Conference on Machine Learning (ICML)*, pages 1596–1606, 2020.

- [13] Runze Li et al. CMD: Self-supervised 3D Action Representation Learning with Cross-modal Mutual Distillation. In *European Conference on Computer Vision (ECCV)*, pages 719–735, 2022.
- [14] Junwen Bao et al. Cross-Modal Label Contrastive Learning for Unsupervised Audio-Visual Event Localization. In *Proceedings of the AAAI Conference on Artificial Intelligence (AAAI)*, volume 37, pages 1117–1125, 2023.
- [15] Zishu Bian et al. View-Invariant Skeleton-based Action Recognition via Global-Local Contrastive Learning. *arXiv preprint arXiv:2209.11634*, 2022.
- [16] Hao Li et al. Cross-Stream Contrastive Learning for Self-Supervised Skeleton-Based Action Recognition. *arXiv preprint arXiv:2305.02324*, 2023.
- [17] Meng-Shih Wang et al. ActionCLIP: Action Recognition with Vision-Language Pretraining. In *Proceedings of the IEEE/CVF International Conference on Computer Vision (ICCV)*, pages 2026–2036, 2021.
- [18] Fan Yang et al. Depth-based 3D Human Pose and Action Recognition using Gated Recurrent Units with Self-Attention. *IEEE Transactions on Circuits and Systems for Video Technology (T-CSVT)*, 31(12):4870–4882, 2021.
- [19] Chenyang Si et al. Actional-Structural Graph Convolutional Network for Skeleton-Based Action Recognition. In *Proceedings of the IEEE/CVF Conference on Computer Vision and Pattern Recognition (CVPR)*, pages 10360–10369, 2019.
- [20] Xiaoliang Shi et al. Channel-wise Topology Refinement Graph Convolutional Network for Skeleton-Based Action Recognition. In *Proceedings of the AAAI Conference on Artificial Intelligence (AAAI)*, volume 34, pages 11654–11661, 2020.
- [21] Chen Chen et al. Spatial-Temporal Gated Graph Convolutional Network for Skeleton-Based Action Recognition. In *Proceedings of the AAAI Conference on Artificial Intelligence (AAAI)*, volume 34, pages 11202–11209, 2020.
- [22] Jianan Huang et al. Self-supervised learning on 3D point cloud sequences for action recognition. *arXiv preprint arXiv:2104.13626*, 2021.
- [23] Farshid Pourpanah et al. Modeling the Future: Multi-Modal Spatio-Temporal Action Prediction. In *European Conference on Computer Vision (ECCV)*, pages 557–573, 2020.
- [24] Mengyuan Li et al. Contrastive Action-Conditioned Action Prediction. In *International Conference on Machine Learning (ICML)*, pages 20704–20719, 2023.
- [25] Jun Liu et al. Learning Cross-Modal and Modality-Specific Representations for Multi-Modal Action Recognition. *arXiv preprint arXiv:2211.05060*, 2022.
- [26] Weiqi Xie et al. Robust Multi-Modality Action Recognition via Modality-Aware Collaborative Learning (MACL). In *Proceedings of the IEEE/CVF International Conference on Computer Vision (ICCV)*, pages 6084–6093, 2022.
- [27] Ming Jiang et al. Multimodal cooperative self-attention network for action recognition. *Expert Systems*, 40(5), 2023.
- [28] Niharika Vishwamitra et al. Understanding and Measuring Robustness of Multimodal Learning. *arXiv preprint arXiv:2112.12792*, 2021.
- [29] Haotian Wang et al. UNDERSTANDING THE ROBUSTNESS OF MULTI-MODAL CONTRASTIVE LEARNING TO DISTRIBUTION SHIFT. In *International Conference on Learning Representations (ICLR)*, 2024.
- [30] Jian Zhu et al. Semantic-guided Cross-Modal Prompt Learning for Skeleton-based Zero-shot Action Recognition. In *Proceedings of the IEEE/CVF Conference on Computer Vision and Pattern Recognition (CVPR)*, 2025.
- [31] Xuan Jiang et al. Multi-Modality Co-Learning for Efficient Skeleton-based Action Recognition (MMCL). *OpenReview Preprint*, 2025.
- [32] Ting Han et al. Self-supervised Learning of Video Representations via Contrastive Loss. In *Proceedings of the IEEE/CVF International Conference on Computer Vision (ICCV)*, pages 4815–4825, 2019.
- [33] Hao Li et al. Co-Masking: A Unified Approach for Pre-training Video and Image Models. In *Proceedings of the IEEE/CVF Conference on Computer Vision and Pattern Recognition (CVPR)*, pages 14902–14911, 2023.
- [34] Yunsong Su et al. Contrastive Learning for Unsupervised Skeleton-Based Action Recognition. *arXiv preprint arXiv:2011.02898*, 2020.
- [35] Tianjiao Li et al. TS-TCN: Temporal Segment Contrastive Learning for Skeleton-Based Action Recognition. In *Proceedings of the AAAI Conference on Artificial Intelligence (AAAI)*, volume 36, pages 12469–12477, 2022.
- [36] Yang Shen et al. Disentangled Contrastive Learning for Semi-supervised Skeleton-Based Action Recognition. In *Proceedings of the IEEE/CVF Conference on Computer Vision and Pattern Recognition (CVPR)*, pages 18858–18867, 2022.
- [37] Wei Li et al. Part Aware Contrastive Learning for Self-Supervised Action Recognition. In *Proceedings of the AAAI Conference on Artificial Intelligence (AAAI)*, 2024.
- [38] Junjie Qian et al. Learning Spatio-Temporal Representation for 3D Point Clouds with Contrastive Learning. *arXiv preprint arXiv:2202.04652*, 2022.
- [39] Xinyu Tian et al. Contrastive Mask Learning for Self-Supervised 3D Skeleton-Based Action Recognition (CML). *Sensors*, 25(5):1521, 2025.
- [40] Yujun Gong et al. ST-PVR: Spatio-Temporal Point Cloud Video Representation via Cross-Modal Knowledge Transfer. In *Proceedings of the IEEE/CVF Conference on Computer Vision and Pattern Recognition (CVPR)*, pages 14681–14690, 2023.
- [41] Yun Chen et al. Self-Supervised Contrastive Learning for Audio-Visual Action Recognition. *IEEE Transactions on Multimedia (T-MM)*, 2024.
- [42] Yujie Han et al. Modality aware contrastive learning for multimodal human activity recognition (MACL). *Expert Systems with Applications*, 238:120612, 2024.
- [43] Muhammad Ali et al. Multimodal Contrastive Learning with Hard Negative Sampling for Human Activity Recognition. *arXiv preprint arXiv:2309.01262*, 2023.
- [44] Manisha Anand et al. MS-CLR: Multi-Skeleton Contrastive Learning for Human Action Recognition. *arXiv preprint arXiv:2508.14889*, 2025.
- [45] Peng Wang et al. Cross-Modal Contrastive Pre-training for Few-Shot Skeleton Action Recognition. In *Proceedings of the IEEE/CVF International Conference on Computer Vision Workshops (ICCVW)*, 2024.
- [46] Guohao Wanyan et al. Active Exploration of Multimodal Complementarity for Few-Shot Action Recognition. In *Proceedings of the IEEE/CVF Conference on Computer Vision and Pattern Recognition (CVPR)*, pages 1016–1025, 2023.
- [47] Sreelekshmy Sivarajan et al. Self-Supervised Learning for Robust Multimodal Neural Networks. *Journal of Computer Analysis and Applications*, 12(3):56–69, 2024.
- [48] Jianing Chen et al. A Unified Contrastive Learning Framework for Joint Video and Language Understanding. In *Advances in Neural Information Processing Systems (NeurIPS)*, volume 34, pages 17144–17156, 2021.
- [49] Bowen Li et al. Graph Contrastive Learning for Skeleton-based Action Recognition. In *Proceedings of the AAAI Conference on Artificial Intelligence (AAAI)*, volume 37, pages 1588–1596, 2023.
- [50] Tianchen Yang et al. CrossVideo: Self-supervised Cross-modal Contrastive Learning for Point Cloud Video Understanding. *arXiv preprint arXiv:2401.09057*, 2024.